

## Impact of ghost loops on dynamical gluon mass generation

---

**Arlene C. Aguilar\***

*Federal University of ABC, CCNH,*

*Rua Santa Adélia 166, CEP 09210-170, Santo André, Brazil*

*E-mail: arlene.aguilar@ufabc.edu.br*

Exploiting the gauge-invariant properties of the PT-BFM truncation scheme for the gluon Schwinger-Dyson equation, we estimate the individual non-perturbative contribution of the “one-loop dressed” ghost loop to the gluon propagator. Using the available quenched lattice data for the gluon and the ghost propagators in  $d = 4$  and  $d = 3$ , we determine how the overall shape of the gluon propagator is affected by the removal of the ghost loop, and what are the consequences on the phenomenon of gluon mass generation.

*International Workshop on QCD Green's Functions, Confinement and Phenomenology,  
September 05-09, 2011  
Trento Italy*

---

\*Speaker.

## 1. Introduction

In the last few years our understanding of the infrared (IR) behavior of the fundamental QCD Green's function has improved substantially. Putting together the information obtained through various non-perturbative methods, such as lattice simulations [1, 2, 3, 4, 5, 6], Schwinger-Dyson equations (SDEs) [7, 8, 9], functional methods [10, 11], and algebraic techniques [13, 14], it is by now well-established that, in the Landau gauge, the gluon propagator and a ghost dressing function are finite in the IR (in  $d = 3, 4$ ). [7, 9]. Evidently, these results support the gluon mass generation picture proposed by Cornwall several years ago [15], disfavoring the so-called “ghost-dominance” picture of QCD [16, 17], whose theoretical cornerstone has been the existence of a divergent (“IR-enhanced”) ghost dressing function.

However, the finiteness of the ghost sector does not imply necessarily that the ghost contribution has been relegated to a marginal role in the QCD dynamics. In fact, compelling evidence to the contrary has emerged from detailed studies of the gap equation that controls the breaking of chiral symmetry and the dynamical generation of a constituent quark mass [18, 19]. Specifically, a detailed study has revealed that the proper inclusion of the ghost sector into the quark SDE is crucial for obtaining quark masses of the order of 300 MeV in the presence of finite gluon propagator [19]

Given the importance of the ghost sector for the dynamical generation of a constituent quark mass, the main purpose of this talk is to ask whether a similar situation applies in the case of the dynamical generation of an effective gluon mass [20].

## 2. Disentangling the “one-loop dressed” ghost contributions

In what follows we will work within the specific framework provided by the synthesis of the pinch technique (PT) [15, 21, 8, 22, 23] with the background field method (BFM) [24].

We start by recalling that within the PT-BFM scheme the gluon self-energy,  $\Pi_{\mu\nu}(q)$ , is given by the sum of the diagrams represented by Fig. 1, i.e.

$$\Pi^{\mu\nu}(q) = \sum_{i=1}^{10} (a_i)^{\mu\nu}. \quad (2.1)$$

Exploiting the well-known blockwise transversality properties of the PT-BFM  $\Pi^{\mu\nu}(q)$ , it is possible to separate the transversal contribution of the one-loop dressed ghost diagrams, represented by the diagrams  $(a_3)$  and  $(a_4)$ , and to be denoted by

$$\Pi_c^{\mu\nu}(q) = (a_3)^{\mu\nu} + (a_4)^{\mu\nu}; \quad (2.2)$$

where  $(a_3)$  and  $(a_4)$  are given by

$$\begin{aligned} (a_3)_{\mu\nu} &= -g^2 C_A \int_k \tilde{\Gamma}_\mu^{(0)}(k, q, -k - q) D(k) D(k + q) \tilde{\Gamma}_\nu(k + q, -q, -k), \\ (a_4)_{\mu\nu} &= 2g^2 C_A g_{\mu\nu} \int_k D(k). \end{aligned} \quad (2.3)$$

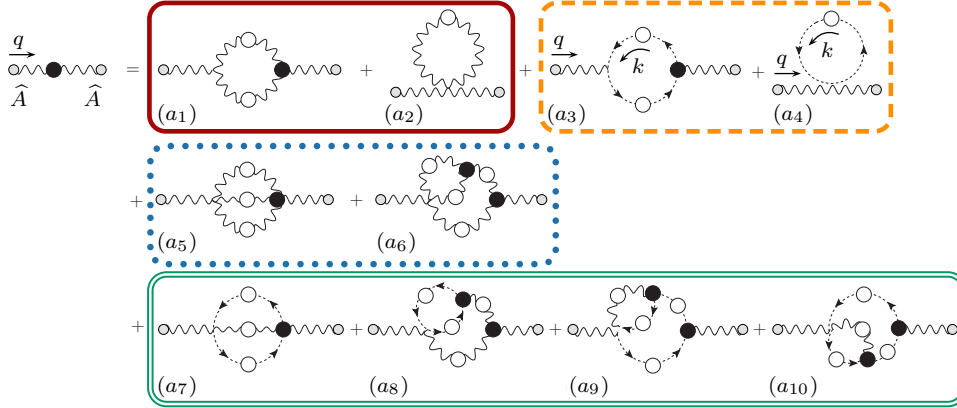


**Figure 1:** The SDE corresponding to the PT-BFM gluon self-energy  $\Pi_{\mu\nu}^{ab}(q)$ . The graphs inside each box furnish an individually transverse contribution. White (black) circles denote full propagators (vertices).

In the equations above,  $D^{ab}(q^2) = \delta^{ab}D(q^2)$  denotes the full ghost propagator, defined in terms of the ghost dressing function  $F(q^2)$  as

$$D(q^2) = \frac{F(q^2)}{q^2}, \quad (2.4)$$

while  $\tilde{\Gamma}_\mu$  represents the three-particle vertex describing the interaction of the background gluon with a ghost and an antighost, with (all momenta entering)

$$i\Gamma_{c^b\hat{A}_\mu^a\tilde{c}^c}(r, q, p) = gf^{acb}\tilde{\Gamma}_\mu(r, q, p); \quad \tilde{\Gamma}_\mu^{(0)}(r, q, p) = (r-p)_\mu. \quad (2.5)$$

Finally,  $C_A$  is the Casimir eigenvalue of the adjoint representation [ $C_A = N$  for  $SU(N)$ ], and we have introduced the  $d$ -dimensional integral measure (in dimensional regularization) according to

$$\int_k \equiv \frac{\mu^\varepsilon}{(2\pi)^d} \int d^d k, \quad (2.6)$$

with  $\mu$  the 't Hooft mass, and  $\varepsilon = 4 - d$ . Then, by virtue of the PT-BFM Ward identity

$$iq^\mu \tilde{\Gamma}_\mu(r, q, p) = D^{-1}(r) - D^{-1}(p), \quad (2.7)$$

it is immediate to establish the transversality of  $\Pi_c^{\mu\nu}(q)$ , namely [22]

$$q_\mu \Pi_c^{\mu\nu}(q) = 0. \quad (2.8)$$

It is convenient for our purposes to decompose the full self-energy  $\Pi_{\mu\nu}(q)$  as

$$\Pi^{\mu\nu}(q) = \Pi_r^{\mu\nu}(q) + \Pi_c^{\mu\nu}(q), \quad (2.9)$$

where  $\Pi_r^{\mu\nu}(q)$  denotes the sum of the remaining subsets of diagrams in Fig. 1, *i.e.*, both the gluon one- and two-loop dressed diagrams, as well as two-loop dressed ghost diagrams,

$$\Pi_r^{\mu\nu}(q) = \sum_{\substack{i=1 \\ i \neq 3,4}}^{10} (a_i)^{\mu\nu}. \quad (2.10)$$

Notice that due to the special Ward identities satisfied by the PT-BFM vertices,  $\Pi_r^{\mu\nu}(q)$  is also transverse [22, 23].

Using Eq. (2.9), the SDE for the full gluon propagator in the Landau gauge of the PT-BFM scheme assumes then the form [7]

$$\Delta^{-1}(q^2)P^{\mu\nu}(q) = \frac{q^2 P^{\mu\nu}(q) + i [\Pi_r^{\mu\nu}(q) + \Pi_c^{\mu\nu}(q)]}{[1 + G(q^2)]^2}, \quad (2.11)$$

where the gluon propagator  $\Delta_{\mu\nu}(q)$  is defined as

$$\Delta_{\mu\nu}(q) = -i\Delta(q^2)P_{\mu\nu}(q); \quad P_{\mu\nu}(q) = g_{\mu\nu} - \frac{q_\mu q_\nu}{q^2}, \quad (2.12)$$

The function  $G$  appearing in (2.11) is the form factor associated with  $g_{\mu\nu}$  in the Lorentz decomposition of the auxiliary two-point function  $\Lambda$ , given by [7, 25]

$$\begin{aligned} \Lambda_{\mu\nu}(q) &= -ig^2 C_A \int_k \Delta_\mu^\sigma(k) D(q-k) H_{\nu\sigma}(-q, q-k, k) \\ &= g_{\mu\nu} G(q^2) + \frac{q_\mu q_\nu}{q^2} L(q^2). \end{aligned} \quad (2.13)$$

Notice that the auxiliary function  $H$  is related to the (conventional) gluon-ghost vertex by the identity

$$\Gamma_\mu(r, q, p) = -p^\nu H_{\nu\mu}(p, r, q), \quad (2.14)$$

and that, in the (background) Landau gauge, the following all order relation holds [26, 27]

$$F^{-1}(q^2) = 1 + G(q^2) + L(q^2). \quad (2.15)$$

Now, let us return to Eq. (2.11), and define in a completely analogous way the quantity  $\Delta_r(q^2)$ , given by

$$\Delta_r^{-1}(q^2)P^{\mu\nu}(q) = \frac{q^2 P^{\mu\nu}(q) + i\Pi_r^{\mu\nu}(q)}{[1 + G(q^2)]^2}. \quad (2.16)$$

Evidently,  $\Delta_r$  represents the propagator obtained by subtracting out from the full propagator  $\Delta$  the one-loop dressed ghost contributions. Then, taking the trace of both Eqs. (2.11) and (2.16), defining the trace of  $\Pi_c^{\mu\nu}(q)$  as

$$\Pi_c(q^2) \equiv \Pi_{c\mu}^\mu(q), \quad (2.17)$$

and solving for  $\Delta_r$ , we arrive at

$$\Delta_r(q^2) = \Delta(q^2) \left\{ 1 - \frac{i\Delta(q^2)\Pi_c(q^2)}{(d-1)[1 + G(q^2)]^2} \right\}^{-1}, \quad (2.18)$$

which represents our master formula.

In order to obtain the behavior of the propagator  $\Delta_r(q^2)$  from Eq. (2.18) we will in the next sections (i) identify the full gluon propagator  $\Delta(q^2)$  with that obtained from the lattice, and (ii) determine nonperturbatively the quantity  $\Pi_c$  from Eqs. (2.3) and (2.17), and evaluate it numerically using as input the lattice results for the ghost dressing function  $F(q^2)$ .

### 3. The nonperturbative calculation of $\Pi_c(q^2)$

The first step in the calculation of the non-perturbative quantity  $\Pi_c(q^2)$  is the definition of an Ansatz for the fully-dressed ghost vertex  $\tilde{\Gamma}_\mu$ , appearing in graph  $(a_3)$  of Eq. (2.3) which satisfies the crucial Ward identity of Eq. (2.7). This task can be accomplished with the help of the “gauge-technique” [28] which reconstruct the vertex by “solving” its Ward identity. Following the same steps of the derivation presented in [29] for the scalar QED vertex, the Ansatz for the fully-dressed ghost vertex  $\tilde{\Gamma}_\mu$ , reads,

$$\tilde{\Gamma}_\mu(r, q, p) = i \frac{(r-p)_\mu}{r^2 - p^2} [D^{-1}(p^2) - D^{-1}(r^2)], \quad (3.1)$$

which evidently satisfies Eq. (2.7) when contracted with  $q^\mu$ . Obviously the “gauge technique” leaves the transverse (automatically conserved) part of the vertex undetermined, which, on general grounds, is expected to be subleading in the IR [28, 30].

Substituting (3.1) in the first equation of (2.3) and taking the trace, it is relatively straightforward to obtain the result

$$\Pi_c(q^2) = g^2 C_A [4T(q) - q^2 R(q)], \quad (3.2)$$

where

$$\begin{aligned} R(q) &= \int_k \frac{D(k+q) - D(k)}{(k+q)^2 - k^2}, \\ T(q) &= \int_k k^2 \frac{D(k+q) - D(k)}{(k+q)^2 - k^2} + \frac{d}{2} \int_k D(k). \end{aligned} \quad (3.3)$$

To further evaluate  $\Pi_c(q^2)$ , we must invoke the so-called “seagull-identity” [31],

$$\int_k k^2 \frac{\partial f(k^2)}{\partial k^2} + \frac{d}{2} \int_k f(k^2) = 0, \quad (3.4)$$

valid in dimensional regularization, which enforces the cancellations of all seagull-type of divergences. Notice that, in the limit  $q \rightarrow 0$ , the term  $q^2 R(q)$  vanishes, and so does  $T(q)$ , since

$$T(q) \xrightarrow{q \rightarrow 0} T(0) = \int_k k^2 \frac{\partial D(k^2)}{\partial k^2} + \frac{d}{2} \int_k D(k) = 0, \quad (3.5)$$

where in the last step we have employed Eq. (3.4), with  $f(k^2) \rightarrow D(k^2)$ . Employing this result, follows immediately from Eq. (3.2) that  $\Pi_c(0) = 0$ . Using the fact that  $\Delta^{-1}(0) = m^2(0)$ , we conclude that the one-loop dressed ghost diagrams  $(a_3)$  and  $(a_4)$  do not contribute *directly* to the value of dynamical gluon mass at zero momentum transfer. The easiest way to appreciate this is by recalling that the mechanism responsible for endowing the gluon with a dynamical mass relies on the presence of massless poles in the nonperturbative tree-gluon [the black circle in graph  $(a_1)$  of Fig. 1], whereas the ghost vertex has the usual structure [note the absence of poles in the Ansatz of Eq. (3.1)] [32].

In addition, notice that when  $d = 4$ ,  $R(q)$  is ultraviolet divergent, and must be properly renormalized, by introducing the appropriate wave-function renormalization constant.

The (subtractive) renormalization must be carried out at the level of (2.11). Specifically (setting directly  $d = 4$ ),

$$\Delta^{-1}(q^2) = \frac{Z_A q^2 + \frac{i}{3} [\Pi_r(q) + \Pi_c(q)]}{[1 + G(q^2)]^2}, \quad (3.6)$$

where the renormalization constant  $Z_A$  is fixed in the MOM scheme through the condition  $\Delta^{-1}(\mu^2) = \mu^2$ . Applying this condition at the level of Eq. (3.6) together with Eq. (2.15), and using the fact that the function  $L(x)$  is considerably smaller than  $G(x)$  in the entire range of momenta, (so that we can use the approximation  $1 + G(\mu^2) \approx F^{-1}(\mu^2) = 1$ ) allows one to express  $Z_A$  as

$$Z_A = 1 - \frac{i}{3\mu^2} [\Pi_r(\mu) + \Pi_c(\mu)]. \quad (3.7)$$

Finally, substituting Eq. (3.7) into Eq. (3.6), and defining (in a natural way) the renormalized  $\Delta_r^{-1}(q^2)$  as

$$\Delta_r^{-1}(q^2) = \frac{q^2 + \frac{i}{3} [\Pi_r(q) - (q^2/\mu^2)\Pi_r(\mu)]}{[1 + G(q^2)]^2}, \quad (3.8)$$

the renormalized version of the master formula (2.18) will read

$$\Delta_r^{-1}(q^2) = \Delta^{-1}(q^2) - \frac{i}{3} \frac{[\Pi_c(q) - (q^2/\mu^2)\Pi_c(\mu)]}{[1 + G(q^2)]^2}. \quad (3.9)$$

Evidently (3.9) is obtained from (2.18) by replacing  $\Delta^{-1}(q^2) \rightarrow \Delta_R^{-1}(q^2)$  (“ $R$ ” for “renormalized”), and  $\Pi_c(q) \rightarrow \Pi_{c,R}(q)$ , where

$$\Pi_{c,R}(q) = \Pi_c(q) - (q^2/\mu^2)\Pi_c(\mu). \quad (3.10)$$

For the ensuing numerical treatment of  $R(q)$  and  $T(q)$  carried out in the next section, it is advantageous to have the crucial property  $T(0) = 0$  a priori built in, in order to avoid possible deviations due to minor numerical instabilities. To that end, we introduce the quantity  $\bar{T}$

$$\bar{T}(q) = T(q) - T(0) = \int_k k^2 \left[ \frac{D(k+q) - D(k)}{(k+q)^2 - k^2} - \frac{\partial D(k)}{\partial k^2} \right], \quad (3.11)$$

which has the property of ensuring (by construction) that  $\bar{T}(0) = 0$ , while, at the same time, coinciding with the original  $T$  for all momenta  $q$ .

In addition, it is convenient to re-express  $R(q)$  and  $\bar{T}(q)$  in terms of the ghost dressing function. Using Eq. (2.4), after some elementary algebra, one obtains

$$R(q) = - \int_k \frac{F(k)}{k^2(k+q)^2} + \int_k \frac{F(k+q) - F(k)}{k^2[(k+q)^2 - k^2]}, \quad \bar{T}(q) = \int_k \left[ \frac{F(k+q) - F(k)}{(k+q)^2 - k^2} - \frac{\partial F(k)}{\partial k^2} \right]; \quad (3.12)$$

note that the angular integration of the first term in  $R$  can be carried out analytically for any value of the space-time dimension  $d$ .

Finally, note that up until this point we have been working in Minkowski space. To make the transition to Euclidean space, we must employ the usual rules. Specifically, we set  $\int_k = i \int_{k_E}$  and  $q_E^2 = -q^2$ , and use that  $\Delta_E(q_E^2) = -\Delta(-q_E^2)$ ;  $F_E(q_E^2) = F(-q_E^2)$ ;  $G_E(q_E^2) = G(-q_E^2)$ , suppressing the subscript “ $E$ ” in what follows.

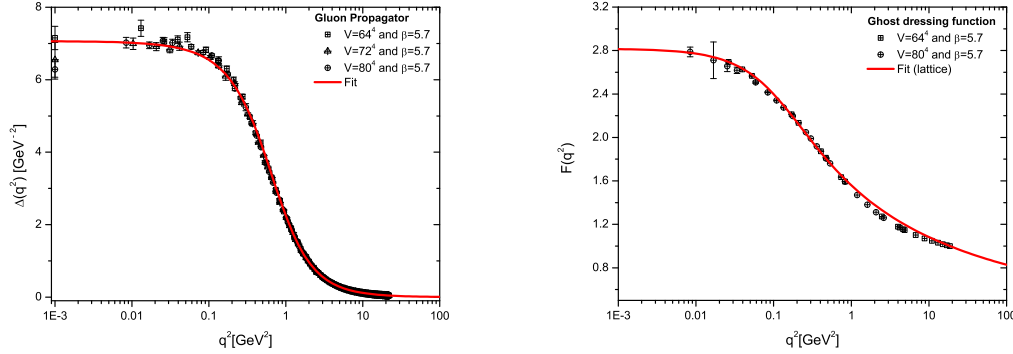


**Figure 2:** *Left panel:* Lattice result for the  $SU(3)$  gluon propagator,  $\Delta(q)$ , in  $d = 4$ , renormalized at  $\mu = 4.3$  GeV. The continuous line represents the fit given by Eq. (4.1). *Right panel:* The  $SU(3)$  ghost dressing function,  $F(q^2)$ , renormalized at the same point,  $\mu = 4.3$  GeV; the solid line corresponds to the fit given by Eq. (4.2).

#### 4. Numerical Results

We will now proceed to perform the numerical analysis. Using the available lattice data on the ghost dressing function  $F$ , we evaluate the terms  $R$  and  $\bar{T}$  given in Eq. (3.12), and combine them following the Eqs. (3.2) and (3.10) to obtain the (renormalized) ghost contribution to the gluon self-energy  $\Pi_c$ . Finally, we construct  $\Delta_r$  using (2.18) and the lattice results available for the gluon propagator  $\Delta$ . This exercise is carried out for two different cases:  $d = 4$ ,  $N = 3$ , and  $d = 3$ ,  $N = 2$ .

In Fig. 2 we show the lattice results for the four-dimensional  $SU(3)$  gluon propagator  $\Delta(q^2)$  (left panel), and the corresponding ghost dressing function  $F(q^2)$  (right panel), obtained from [3], and renormalized at  $\mu = 4.3$  GeV.

As has been discussed in detail in the literature [19, 32, 33], both sets of data can be accurately fitted in terms of IR-finite quantities. More specifically, for the case of  $\Delta(q^2)$ , we have proposed a fit of the form [33]

$$\Delta^{-1}(q^2) = M^2(q^2) + q^2 \left[ 1 + \frac{13C_A g_1^2}{96\pi^2} \ln \left( \frac{q^2 + \rho_1 M^2(q^2)}{\mu^2} \right) \right], \quad M^2(q^2) = \frac{m_0^4}{q^2 + \rho_2 m_0^2}. \quad (4.1)$$

Notice that in the above expression, the finiteness of  $\Delta^{-1}(q^2)$  is assured by the presence of the function  $M^2(q^2)$ , which forces the value of  $\Delta^{-1}(0) = M^2(0) = m_0^2/\rho_2$ . The continuous line on the left panel of Fig. 2 corresponds our best fit, which can be reproduced setting  $m_0 = 520$  MeV,  $g_1^2 = 5.68$ ,  $\rho_1 = 8.55$  and  $\rho_2 = 1.91$ .

The  $SU(3)$  lattice data for  $F(q^2)$ , shown in the right panel of Fig. 2, will be fitted by the following expression

$$F^{-1}(q^2) = 1 + \frac{9}{4} \frac{C_A g_1^2}{48\pi^2} \ln \left( \frac{q^2 + \rho_3 M^2(q^2)}{\mu^2} \right); \quad M^2(q^2) = \frac{m_0^4}{q^2 + \rho_4 m_0^2}, \quad (4.2)$$

with the parameters given by  $m_0 = 520$  MeV,  $g_2^2 = 8.65$ ,  $\rho_3 = 0.25$  and  $\rho_4 = 0.64$ . Notice that the  $M(q^2)$  has the same power-law running as the one reported in Refs [34, 35, 36].

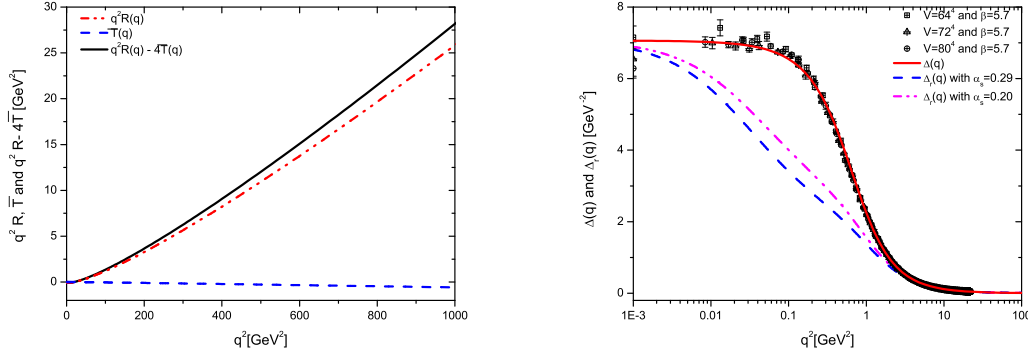


**Figure 3:** *Left panel:* Numerical evaluation of the ghost contribution  $\Pi_c(q)$  to the gluon propagator using as input our best fit for the  $d = 4$ ,  $N = 3$  ghost dressing lattice data. *Right panel:* The removal of the one-loop dressed ghost contribution from the (lattice) gluon propagator results in a diminished “swelling” in the momentum region below 1 GeV<sup>2</sup>.

The only missing ingredient for the actual nonperturbative determination of  $\Pi_c$ , and therefore  $\Delta_r$ , is the value of  $\alpha_s = g^2/4\pi$ . Instead of choosing a single value for  $\alpha_s$ , we will use the physically motivated range of values  $[0.20, 0.29]$ , which will furnish a more representative picture of the numerical impact of the ghost corrections on the gluon propagator.

The results obtained for the renormalized  $R$  and  $\bar{T}$ , after substituting into the corresponding formulas our best fit for  $F$ , given by Eq. (4.2), are shown on the left panel of Fig. 3, together with the combination  $q^2 R - 4\bar{T}$ , which appears on the rhs of Eq. (3.2). It is clear that the contribution of the term  $4\bar{T}$  is rather negligible; in a way this is to be expected, given that this term vanishes identically in perturbation theory (for all values of  $q$ ), and vanishes nonperturbatively at the origin.

Next, we use these results to construct  $\Pi_c$ , given in Eq. (3.10), and finally  $\Delta_r$ , expressed by Eq. (3.9) (Fig. 3 right panel), using both values of  $\alpha_s$ , namely  $\alpha_s = 0.29$  (blue dashed line) and  $\alpha_s = 0.20$  (magenta dashed-dotted line).

We then see that the net effect of removing the ghost contribution is to suppress significantly the support of the gluon propagator in the region below 1 GeV<sup>2</sup>. Higher values of  $\alpha_s$  increase the impact of the ghost contributions, but only slightly, as can be seen on the right panel of Fig. 3. As we will see in the next section, this “deflating” of the gluon propagator in the intermediate region of momenta, produced by the removal of the ghost contributions, has far-reaching consequences on the generation of a dynamical gluon mass.

Now we will repeat the same exercise using the lattice results for  $d = 3$  and  $N = 2$ . Let us start, as in the previous case, by showing in Fig. 4 the lattice results [2] for the three-dimensional gluon propagator  $\Delta(q)$  (left panel) and the ghost dressing function  $F(q)$  (right panel). Both  $\Delta(q)$  and  $F(q)$  saturate in the deep IR region, and can therefore be fitted by means of IR finite expressions.

In the case of the gluon propagator, an accurate fit is giving by

$$\Delta(q) = A \exp \left[ -(q - q_0)^2 / w \right] + \frac{1}{a + bq + cq^2}, \quad (4.3)$$

where the fitting parameters are  $A = 0.49$ ,  $q_0 = 0.11$ ,  $w = 0.37$ ,  $a = 0.43$ ,  $b = -0.85$ , and  $c = 1.143$ .



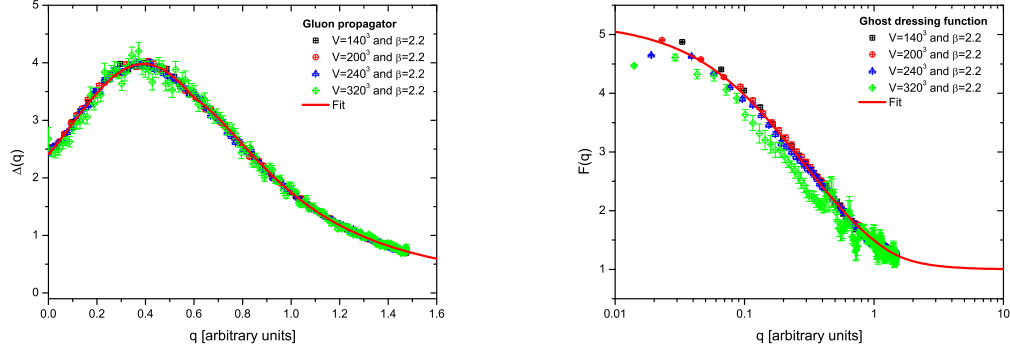


**Figure 4:** *Left panel:* Lattice results for the  $SU(2)$  gluon propagator in  $d = 3$ . The continuous line represents our best fit to the data obtained from Eq. (4.3). *Right panel:* Lattice data for the  $SU(2)$  ghost dressing function  $F(q)$  in 3 dimensions; the solid line corresponds to the best fit given by Eq. (4.4).

For the ghost dressing function, we use the following piecewise interpolator

$$F(q) = \frac{1}{a + bq + cq^2}, \text{ for } q^2 \leq 3 \quad \text{and} \quad F(q) = 1 + \frac{d}{eq + q^2}, \text{ for } q^2 > 3, \quad (4.4)$$

with fitting coefficients  $a = 0.19$ ,  $b = 0.61$ ,  $c = -0.14$ ,  $d = 0.63$  and  $e = 0.26$  obtained by requiring the function to be continuous at  $q^2 = 3$ .

Next, substituting the results presented on the left panel of Fig. 5 into Eqs. (3.2) and (2.18), and using  $g = 1.208$ , we compute  $\Pi_c$  and  $\Delta_r$ . On the right panel of Fig. 5, we compare the residual propagator  $\Delta_r$  (blue dashed line) with the full propagator  $\Delta(q)$ . Clearly, the effect in the tridimensional case is even more pronounced: the ghost contribution completely dominates over the rest, determining to a large extent the overall shape and structure of the propagator.

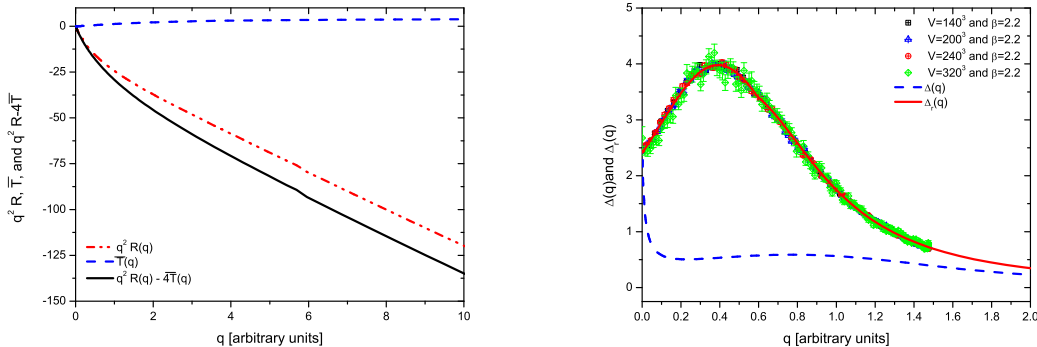


**Figure 5:** *Left panel:* Numerical evaluation of the ghost contribution  $\Pi_c$  to the gluon propagator using as input our best fit for the  $d = 3$ ,  $N = 2$  ghost dressing lattice data. *Right panel:* The result of removing the one-loop dressed ghost contribution from the gluon propagator in  $d = 3$ . The effect is much more dramatic than in the  $d = 4$  case, since all the structure is determined by the ghost contribution, while  $\Delta_r$  has the sole (but crucial!) role of rendering the propagator finite at  $q = 0$ .

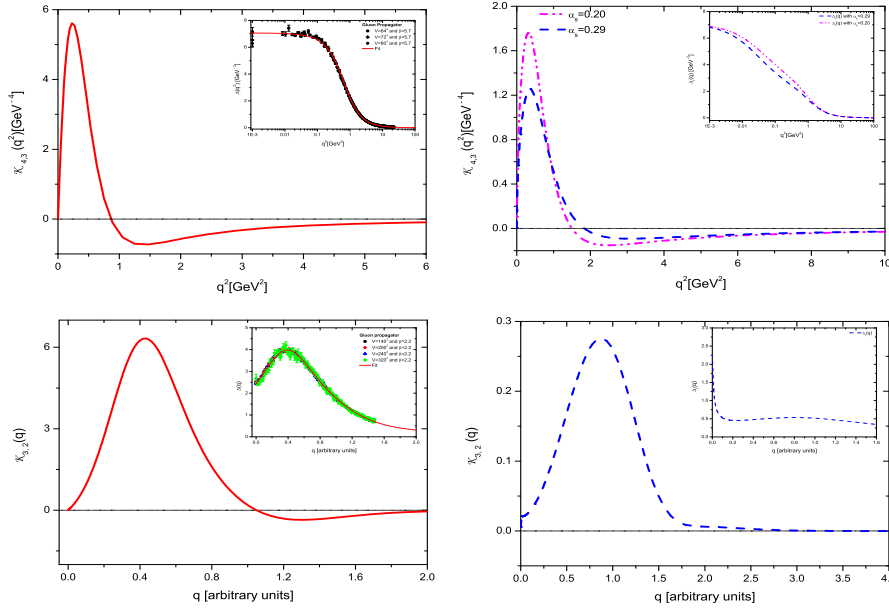


**Figure 6:** The kernel  $\mathcal{K}_{d,N}$  of Eq. (5.2) constructed out of the lattice propagator  $\Delta$  (left panels) and the ghost-less propagator  $\Delta_r$  (right panels) for the  $d = 4, N = 3$  (top row), and  $d = 3, N = 2$  (bottom row) cases. The insets show in each case the shape of the propagator used to evaluate the kernels.

## 5. The effects of the ghost loop in the mass equation

In the previous section we have studied how the subtraction of the ghost contributions affects the profile of the gluon propagator. However, as we will see now, the effects goes way beyond a simple change in the overall propagator shape, modifying its salient qualitative characteristics, and in particular the generation of a dynamical gluon mass.

To establish this, we use the  $q \rightarrow 0$  limit of the equation describing the behavior of the dynamical mass equation, *i.e.*

$$m^2(0) = -\frac{d-1}{d(4\pi)^{\frac{d}{2}}\Gamma(\frac{d}{2})} \frac{4g^2 C_A}{1+G(0)} \int_0^\infty dy m^2(y) \mathcal{K}_{d,N}(y), \quad (5.1)$$

with the kernel  $\mathcal{K}_{d,N}$  given by

$$\mathcal{K}_{d,N}(y) = y^{\frac{d}{2}-1} \Delta(y) [y\Delta(y)]'. \quad (5.2)$$

Since the constant multiplying the integral is positive, the negative sign in front of Eq. (5.1) tells us that the required physical constraint  $m^2(0) > 0$  can be fulfilled if and only if the integral kernel  $\mathcal{K}_{d,N}$  (constructed solely out of the gluon propagator) displays a sufficiently deep and extended negative region at intermediate momenta [32].

In the left panels of Fig. 6 we plot the kernels  $\mathcal{K}_{d,N}$  obtained from the lattice data for the cases  $d = 4, N = 3$  (top row), and  $d = 3, N = 2$  (bottom row); both display the characteristic negative region that allows, at least in principle, the existence of solutions of Eq. (5.1), furnishing a positive value for  $m^2(0)$ .

On the other hand, the situation changes substantially once the ghost loop is removed, in which case the kernels  $\mathcal{K}_{d;N}$  must be constructed from  $\Delta_r$  (right panels of the same figure). For  $d = 4$  one observes a shift towards higher  $qs$  of the zero crossing, and a correspondingly suppressed negative region; even though this is not sufficient to exclude *per se* the existence of a physical solution to the mass equation (5.1), a thorough study of the approximate equation derived in [32] reveals that no physical solution may be found. The  $d = 3$  situation is even more obvious: the highly suppressed negative region present in this case cannot support solutions of (5.1) with  $m^2(0) > 0$ , thus leaving as the only possibility the trivial  $m^2 = 0$  solution.

The main conclusion one can draw, therefore, is that the ghosts play a fundamental role in the mechanism of dynamical gluon mass generation, since the failure to properly include them results in the inability of the theory to generate dynamically a mass for the gluon.

## 6. Conclusions

In this talk we have presented a study of the impact of the ghost sector on the overall form of the gluon propagator in a pure Yang-Mills theory, for different space-time dimensions ( $d = 3, 4$ ) and  $SU(N)$  gauge groups ( $N = 2, 3$ ).

The suppression of the gluon propagator induced by the removal of the ghost-loops has far-reaching consequences on the mechanism that endows gluons with a dynamical mass, associated with the observed IR-finiteness of the gluon propagator and the ghost-dressing function. Specifically, using a recently derived integral equation controlling the dynamics of the (momentum-dependent) gluon mass, we have demonstrated that when the reduced gluon propagators are used as inputs, the corresponding kernels are modified in such a way that no physical solutions may be found, thus failing to generate a mass gap for the pure Yang-Mills theory [20]. Instead, as has been shown in [32], the use of the full gluon propagator in the same equation generates a physically acceptable gluon mass.

## Acknowledgments

I would like to thank the ECT\* for the hospitality and for supporting the QCD-TNT II organization. This work was supported by Fundação de Amparo à Pesquisa do Estado de São Paulo (Fapesp) under grant 2011/11474-8 and by the Brazilian Funding Agency CNPq - grant 305850/2009-1.

## References

- [1] A. Cucchieri and T. Mendes, PoS **LAT2007**, 297 (2007); Phys. Rev. Lett. **100**, 241601 (2008).
- [2] A. Cucchieri, T. Mendes and A. R. Taurines, Phys. Rev. D **67**, 091502 (2003).
- [3] I. L. Bogolubsky, E. M. Ilgenfritz, M. Muller-Preussker and A. Sternbeck, PoS **LATTICE**, 290 (2007).
- [4] O. Oliveira, P. J. Silva, Phys. Rev. **D79**, 031501 (2009); PoS **LAT2009**, 226 (2009).
- [5] H. Suganuma, T. Iritani, A. Yamamoto and H. Iida, PoS **QCD -TNT09**, 044 (2009); PoS **LATTICE 2010**, 289 (2010).

- [6] P. O. Bowman *et al.*, Phys. Rev. D **76**, 094505 (2007).
- [7] A. C. Aguilar, D. Binosi and J. Papavassiliou, Phys. Rev. D **78**, 025010 (2008); A. C. Aguilar, D. Binosi and J. Papavassiliou, Phys. Rev. D **81**, 125025 (2010).
- [8] D. Binosi and J. Papavassiliou, Phys. Rept. **479**, 1-152 (2009).
- [9] Ph. Boucaud, J. P. Leroy, A. L. Yaouanc, J. Micheli, O. Pene and J. Rodriguez-Quintero, JHEP **0806** (2008) 012.
- [10] J. Braun, H. Gies and J. M. Pawłowski, Phys. Lett. B **684**, 262 (2010).
- [11] A. P. Szczepaniak and H. H. Matevosyan, Phys. Rev. D **81**, 094007 (2010).
- [12] D. Zwanziger, Nucl. Phys. B **412**, 657 (1994).
- [13] D. Dudal, J. A. Gracey, S. P. Sorella, N. Vandersickel and H. Verschelde, Phys. Rev. D **78**, 065047 (2008).
- [14] K. -I. Kondo, Phys. Rev. D **84**, 061702 (2011).
- [15] J. M. Cornwall, Phys. Rev. D **26**, 1453 (1982).
- [16] R. Alkofer, L. von Smekal, Phys. Rept. **353**, 281 (2001).
- [17] D. Zwanziger, Phys. Rev. **D65**, 094039 (2002).
- [18] C. S. Fischer, R. Alkofer, Phys. Rev. **D67**, 094020 (2003).
- [19] A. C. Aguilar and J. Papavassiliou, Phys. Rev. D **83**, 014013 (2011).
- [20] A. C. Aguilar, D. Binosi and J. Papavassiliou, arXiv:1108.5989 [hep-ph].
- [21] J. M. Cornwall and J. Papavassiliou, Phys. Rev. D **40**, 3474 (1989).
- [22] A. C. Aguilar and J. Papavassiliou, JHEP **0612**, 012 (2006).
- [23] D. Binosi and J. Papavassiliou, Phys. Rev. D **77**(R), 061702 (2008); JHEP **0811**, 063 (2008).
- [24] See, e.g., L. F. Abbott, Nucl. Phys. B **185**, 189 (1981), and references therein.
- [25] A. C. Aguilar, D. Binosi, J. Papavassiliou and J. Rodriguez-Quintero, Phys. Rev. D **80**, 085018 (2009).
- [26] P. A. Grassi, T. Hurth and A. Quadri, Phys. Rev. D **70**, 105014 (2004).
- [27] A. C. Aguilar, D. Binosi and J. Papavassiliou, JHEP **0911**, 066 (2009).
- [28] A. Salam, Phys. Rev. **130**, 1287 (1963); A. Salam and R. Delbourgo, Phys. Rev. **135**, B1398 (1964); R. Delbourgo and P. C. West, J. Phys. A **10**, 1049 (1977); R. Delbourgo and P. C. West, Phys. Lett. B **72**, 96 (1977).
- [29] J. S. Ball, T. -W. Chiu, Phys. Rev. **D22**, 2542 (1980).
- [30] A. Kizilersu and M. R. Pennington, Phys. Rev. D **79**, 125020 (2009); A. Bashir, A. Kizilersu and M. R. Pennington, Phys. Rev. D **57**, 1242 (1998).
- [31] A. C. Aguilar and J. Papavassiliou, Phys. Rev. D **81**, 034003 (2010).
- [32] A. C. Aguilar, D. Binosi and J. Papavassiliou, Phys. Rev. D **84**, 085026 (2011).
- [33] A. C. Aguilar, D. Binosi, J. Papavassiliou, JHEP **1007**, 002 (2010).
- [34] M. Lavelle, Phys. Rev. **D44**, 26-28 (1991).
- [35] A. C. Aguilar, J. Papavassiliou, Eur. Phys. J. **A35**, 189-205 (2008).
- [36] O. Oliveira, P. Bicudo, J. Phys. G **G38**, 045003 (2011).